Energy and helicity preserving schemes for hydro- and magnetohydro-dynamics flows with symmetry

Jian-Guo Liu [a], Wei-Cheng Wang [b,*]

[a] *Department of Mathematics, Institute for Physical Science and Technology, University of Maryland, College Park, MD 20742, USA*
[b] *Department of Mathematics, National Tsing Hua University, Hsinchu, Hsinchu 300, Taiwan*

Received 23 July 2003; received in revised form 12 December 2003; accepted 21 March 2004
Available online 27 April 2004

Abstract

We propose a class of simple and efficient numerical scheme for incompressible fluid equations with coordinate symmetry. By introducing a generalized vorticity-stream formulation, the divergence free constraints are automatically satisfied. In addition, with explicit treatment of the nonlinear terms and local vorticity boundary condition, the Navier–Stokes (MHD, respectively) equation essentially decouples into 2 (4, respectively) scalar equation and thus the scheme is very efficient. Moreover, with proper discretization of the nonlinear terms, the scheme preserves both energy and helicity identities numerically. This is achieved by recasting the nonlinear terms (convection, vorticity stretching, geometric source, Lorentz force and electro-motive force) in terms of Jacobians. This conservative property is valid even in the presence of the pole singularity for axisymmetric flows. The exact conservation of energy and helicity has effectively eliminated excessive numerical viscosity. Numerical examples have demonstrated both accuracy and efficiency of the scheme. Finally, local mesh refinement near the boundary can also be easily incorporated into the scheme without extra cost.
© 2004 Elsevier Inc. All rights reserved.

AMS: 65N06; 65N35; 35J05

Keywords: Energy; Helicity; Jacobian; Permutation identity; Axisymmetric flow; Navier–Stokes; MHD

1. Introduction

In the numerical simulation of incompressible flows, it is desirable to have exact numerical conservation of physically conserved quantities such as the energy and the helicity. The conservation of physical quantities not only provides a diagnostic check for physically relevant numerical solutions, it also guarantees that the numerical scheme is nonlinearly stable and free from excessive numerical viscosity. This is

* Corresponding author.
E-mail addresses: jliu@math.umd.edu (J.-G. Liu), wangwc@math.nthu.edu.tw (W.-C. Wang).

0021-9991/$ - see front matter © 2004 Elsevier Inc. All rights reserved.
doi:10.1016/j.jcp.2004.03.005

essential for large time direct numerical simulations as well as the numerical search for possible flow singularities.

Preserving energy numerically for incompressible Navier–Stokes equation has been quite common in many numerical methods. For examples, a well known trick to obtain the conservation of energy is by averaging a conservative and a non-conservative discretization of the nonlinear convection term. However, it is usually difficult to satisfy two or more physical conservation laws numerically. The classical Arakawa scheme preserves both energy and enstrophy (mean square of the vorticity) for 2D incompressible Euler equation. This result was generalized recently to a high order discontinuous Galerkin method [8]. A strong convergence result was also obtained for this scheme [11] when the initial value of the vorticity is merely square-integrable. Some important flows such as vortex patches belong to this class.

For general three dimensional flows, enstrophy is no longer a conserved quantity. Instead, there is a conservation law for the helicity. Although the discovery of this conservation law is only a recent event (Moreau, 1961 [14]), it has played an important role in modern research on vortex dynamics for fluids and plasma. The helicity has an interesting topological interpretation in terms of total circulations and Gauss linking number of two interlocking vortex filaments. A comprehensive review of this subject can be found in Moffatt [13]. Although there is at present no numerical method preserving both helicity and energy, the conservation of the energy and cross helicity for three dimensional MHD has already been obtained in a recent work by the authors [9]. On a set of dual staggered grids, the classic MAC scheme for Navier–Stokes equation [6] and Yee's scheme for Maxwell equation [17] are combined with particular care on discretization of the nonlinear terms. The divergence free condition for both the velocity field and the magnetic field are maintained in the MAC–Yee scheme [9].

In this paper, we take a different approach and focus on three dimensional flows with coordinate symmetry. Pipe flows and axisymmetric flows are two typical examples. For such symmetric flows, we introduce a generalized vorticity-stream formulation, thus the divergence free constraint for the fluid velocity is automatically satisfied. Under this vorticity-stream formulation, all the nonlinear terms (convection, vorticity stretching, geometric source, Lorentz force and electro-motive force) for the Navier–Stokes and MHD equation can be recast as Jacobians. Associated with the Jacobians we introduce a trilinear form equipped with a permutation identity which leads naturally to the conservation of energy and helicities for both the Navier–Stokes and MHD equation. We then device a recipe of preserving the permutation identities numerically and hence the energy and helicities. As an illustration, we implement a simple second order finite difference scheme based on centered difference in space and high order Runge–Kutta in time. The scheme is very efficient since the nonlinear terms are treated explicitly and a local vorticity boundary condition similar to Thom's formula [3,16] is applied to update the vorticity at the physical boundary. The system therefore decouples into several scalar equations. On the other hand, since the energy and helicities are preserved exactly, the scheme is free from excess numerical viscosity and therefore very accurate. Another advantage of the scheme is the flexibility of choosing coordinate system since our formulation is coordinate-independent. Mesh refinement near the boundary can be built into the equation by stretching the coordinate with essentially no extra cost. The treatment of the nonlinear terms can be generalized to higher order finite difference, finite element and spectral methods following the same guideline.

In practical implementations, the coordinate systems associated with these symmetric flows often exhibits coordinate singularities such as the symmetry axis in cylindrical coordinate systems and the origin in polar coordinates. A well known trick to handle this situation is to shift the grid points half grid away from the singularity [12]. Remarkably, the permutation identity and therefore the energy and helicity conservation remains valid even in the presence of the pole singularity for axisymmetric flows.

It is worth noting that the energy and helicity preserving scheme (EHPS) here and the MAC–Yee scheme in [9] are based on totally different approaches. The MAC–Yee scheme is a second order finite difference scheme for fully 3D MHD equation in primitive variables. The divergence free constraint is enforced by means of staggered grids and exact discrete Hodge decomposition. The energy and the cross helicity are

preserved numerically through proper averaging in the evaluation of nonlinear terms. The magnetic helicity is not preserved numerically since the magnetic field and the magnetic potential are not defined on the same set of grids. In contrast, EHPS applies to 3D Navier–Stokes and MHD flows with symmetry, which admits a generalized vorticity-stream formulation. All the energy and helicities are conserved locally. This is achieved by recasting the nonlinear terms as Jacobians and realizing the permutation identity for the Jacobians numerically. This realization does not require staggered grids and is not restricted to second order finite difference schemes.

The rest of this paper is organized as follows: In Section 2, we recall the energy and helicity identities for general 3D flows. In Section 3, we introduce the generalized vorticity-stream formulation for symmetric flows and derive the expression of the nonlinear terms as Jacobians. In Section 4, we introduce the permutation identity for the Jacobian and re-derive the energy and helicity identities from the permutation identity. We then introduce EHPS by discretizing the nonlinear terms in such a way that the permutation identity is preserved numerically. In Section 5, we give more details on the implementation of finite difference EHPS for axisymmetric flows including the treatment of the pole singularity and the physical boundary conditions. Finally we give several numerical examples in Section 6 and a few concluding remarks in Section 7. The derivation of the energy and helicity identities for the MHD equation and some technical proof regarding the numerical boundary condition for physical boundaries are given in the Appendix A.

2. Energy and helicity conservation laws for 3D flows

The incompressible Navier–Stokes equation on a region $D \subseteq \mathbb{R}^3$ can be written as

$$\begin{aligned} &\partial_t \boldsymbol{u} + \boldsymbol{\omega} \times \boldsymbol{u} + \nabla \tilde{p} = -\nu \nabla \times \boldsymbol{\omega} \\ &\nabla \cdot \boldsymbol{u} = 0, \end{aligned} \tag{2.1}$$

with no-slip boundary condition

$$\boldsymbol{u} = \boldsymbol{0} \quad \text{on } \partial D, \tag{2.2}$$

where $\tilde{p} = p + |\boldsymbol{u}|^2/2$ is the total pressure.

Eq. (2.1) involves only elementary grad, div, curl and the cross product of vector fields. It is therefore suitable to work with in any curvilinear orthogonal coordinate system and much simplifies our derivation below.

Similarly, we can write the 3D incompressible MHD equation as

$$\begin{aligned} &\partial_t \boldsymbol{u} + \boldsymbol{\omega} \times \boldsymbol{u} + \nabla \tilde{p} = -\nu \nabla \times \boldsymbol{\omega} + \alpha \boldsymbol{j} \times \boldsymbol{b}, \\ &\nabla \cdot \boldsymbol{u} = 0, \\ &\partial_t \boldsymbol{b} = -\eta \nabla \times \boldsymbol{j} + \nabla \times (\boldsymbol{u} \times \boldsymbol{b}), \\ &\boldsymbol{\omega} = \nabla \times \boldsymbol{u}, \quad \boldsymbol{j} = \nabla \times \boldsymbol{b}, \end{aligned} \tag{2.3}$$

with no-slip and perfectly conducting wall conditions

$$\boldsymbol{u} = \boldsymbol{0}, \quad \boldsymbol{j} \times \boldsymbol{n} = \boldsymbol{0} \quad \text{on } \partial D. \tag{2.4}$$

Here $\boldsymbol{u}$ is the fluid velocity, $\boldsymbol{\omega}$ is the vorticity, $\tilde{p}$ is the total pressure, $\boldsymbol{b}$ is the magnetic field, $\boldsymbol{j}$ is the electric current density and $\boldsymbol{n}$ is the outward normal. The parameters ν^{-1}, η^{-1} and $\alpha^{-1/2}$ are usually referred to as the fluid Reynolds number, the magnetic Reynolds number and the Alfvén number, respectively.

The conserved quantities are made transparent by the expression of the nonlinear term in (2.1). Since $\boldsymbol{\omega} \times \boldsymbol{u}$ is perpendicular to both $\boldsymbol{\omega}$ and $\boldsymbol{u}$, it follows that

$$\int_D \boldsymbol{u}\cdot\partial_t\boldsymbol{u} + \int_D \boldsymbol{u}\cdot\nabla\tilde{p} = -\nu\int_D \boldsymbol{u}\cdot\nabla\times\boldsymbol{\omega} \tag{2.5}$$

and

$$\int_D \boldsymbol{\omega}\cdot\partial_t\boldsymbol{u} = -\nu\int_D \boldsymbol{\omega}\cdot\nabla\times\boldsymbol{\omega}. \tag{2.6}$$

In view of the no-slip boundary condition (2.2) and the following identity

$$\nabla\cdot(\boldsymbol{u}\times\boldsymbol{\omega}) = \boldsymbol{\omega}\cdot(\nabla\times\boldsymbol{u}) - \boldsymbol{u}\cdot(\nabla\times\boldsymbol{\omega}), \tag{2.7}$$

we have

$$-\nu\int_D \boldsymbol{u}\cdot\nabla\times\boldsymbol{\omega} = -\nu\int_D \boldsymbol{\omega}\cdot\boldsymbol{\omega}, \tag{2.8}$$

$$\int_D \boldsymbol{\omega}\cdot\partial_t\boldsymbol{u} = \int_D \boldsymbol{u}\cdot\partial_t\boldsymbol{\omega} = \frac{1}{2}\frac{\mathrm{d}}{\mathrm{d}t}\int_D \boldsymbol{u}\cdot\boldsymbol{\omega} \tag{2.9}$$

and the conservation of energy and helicity follows:

$$\frac{\mathrm{d}}{\mathrm{d}t}\frac{1}{2}\int_D |\boldsymbol{u}|^2 = -\nu\int_D |\boldsymbol{\omega}|^2, \tag{2.10}$$

$$\frac{\mathrm{d}}{\mathrm{d}t}\frac{1}{2}\int_D \boldsymbol{u}\cdot\boldsymbol{\omega} = -\nu\int_D \boldsymbol{\omega}\cdot(\nabla\times\boldsymbol{\omega}). \tag{2.11}$$

For inviscid flows, the helicity $\int_D \boldsymbol{u}\cdot\boldsymbol{\omega}$ is invariant in time. It has an intrinsic topological interpretation of the flow. For example, when the flow pattern is two knotted vortex tubes or vortex filaments, the helicity is then equal to $\pm 2n\Phi_1\Phi_2$, where Φ_1 and Φ_2 are the circulation in the cross section of the vortex tubes respectively, and n is the Gauss linking number [13].

The conservation of energy, cross helicity and magnetic helicity for the MHD equation (2.3) can be derived similarly. See Appendix A for details.

3. Generalized vorticity-stream formulation for symmetric flows

This paper is motivated by the work of Grauer and Sideris [5] in the numerical search of possible singularities for the axisymmetric solutions of the Euler equation. For axisymmetric flows, the velocity and the vorticity can be written as

$$\boldsymbol{u} = (0,0,u) + \nabla\times(0,0,\psi), \qquad \boldsymbol{\omega} = (0,0,\omega) + \nabla\times(0,0,u), \tag{3.1}$$

and the Euler equation reduces to

$$\begin{aligned} &\partial_t u + (u_x\partial_x + u_r\partial_r)u + \frac{u_r}{r}u = 0,\\ &\partial_t\omega + (u_x\partial_x + u_r\partial_r)\omega - \frac{u_r}{r}\omega = \frac{1}{r}\partial_x(u^2),\\ &-\nabla^2\psi + \frac{1}{r^2}\psi = \omega, \end{aligned} \tag{3.2}$$

where

$$u_r = -\partial_x \psi, \quad u_x = \partial_r \psi + \frac{\psi}{r}. \tag{3.3}$$

The formulation (3.1) and (3.2) can be generalized to general 3D flows with coordinate symmetry.

By symmetry, we mean that both the physical domain and the solution are invariant under translation in a coordinate direction. To be more precise, let $\boldsymbol{X} = (x_1, x_2, x_3)$ be the Cartesian coordinate system and $\boldsymbol{Y} = (y_1, y_2, y_3)$ a curvilinear orthogonal coordinate system with unit vectors $(\boldsymbol{e}_1, \boldsymbol{e}_2, \boldsymbol{e}_3)$. Denote by h_i, $i = 1, 2, 3$, the local stretching factors given by $\mathrm{d}\boldsymbol{X} = \sum_j h_j dy_j \boldsymbol{e}_j$. The three basic differential operators are given by

$$\nabla f = \left(\frac{1}{h_1}\partial_1 f, \frac{1}{h_2}\partial_2 f, \frac{1}{h_3}\partial_3 f \right), \tag{3.4}$$

$$\nabla \cdot \boldsymbol{f} = \frac{1}{h_1 h_2 h_3} (\partial_1 (h_2 h_3 f_1) + \partial_2 (h_1 h_3 f_2) + \partial_3 (h_1 h_2 f_3)), \tag{3.5}$$

$$\nabla \times \boldsymbol{f} = \frac{1}{h_1 h_2 h_3} \begin{vmatrix} h_1 \boldsymbol{e}_1 & h_2 \boldsymbol{e}_2 & h_3 \boldsymbol{e}_3 \\ \partial_1 & \partial_2 & \partial_3 \\ h_1 f_1 & h_2 f_2 & h_3 f_3 \end{vmatrix}. \tag{3.6}$$

If we denote by y_3 the direction of translation invariance, then by symmetry we mean that the active independent variables are defined on the cross section, $(y_1, y_2) \in \Omega$, and that both h_i and the fluid variables are independent of y_3. That is, $h_i = h_i(y_1, y_2)$, $i = 1, 2, 3$ and $\partial_3 \equiv 0$.

For simplicity of presentation, we have assumed that y_i are mutually orthogonal in our derivation. In fact, we are interested in the case where y_3 is orthogonal to the cross section Ω (such as pipe flows and axisymmetric flows, for example). The orthogonality between y_1 and y_2 is not essential, see Remark 2 in Section 5.

For a symmetric incompressible velocity field $\boldsymbol{u} = \boldsymbol{u}(y_1, y_2)$

$$\nabla \cdot \boldsymbol{u} = \frac{1}{h_1 h_2 h_3} (\partial_1 (h_2 h_3 u_1) + \partial_2 (h_3 h_1 u_2)) = 0, \tag{3.7}$$

with $\boldsymbol{u} \cdot \boldsymbol{n}|_{\partial\Omega} = 0$, we can always introduce a potential ψ, the component of the stream vector in the symmetry direction, such that

$$\partial_2 (h_3 \psi) = h_2 h_3 u_1, \qquad \partial_1 (h_3 \psi) = -h_3 h_1 u_2, \tag{3.8}$$

and we can write

$$\boldsymbol{u} = \left(\frac{1}{h_3} \frac{\partial_2 (h_3 \psi)}{h_2}, -\frac{1}{h_3} \frac{\partial_1 (h_3 \psi)}{h_1}, u \right) = (0, 0, u) + \nabla \times (0, 0, \psi). \tag{3.9}$$

Here $u = u_3$ is the velocity component in the symmetry direction. For axisymmetric flows, u is known as the swirling velocity. Direct computation leads to

$$\nabla \times \nabla \times (0, 0, \psi) = (0, 0, \mathscr{L}\psi), \tag{3.10}$$

where

$$\mathscr{L}\psi = -\frac{1}{h_1 h_2} \left(\partial_1 \left(\frac{h_2}{h_1 h_3} \partial_1 (h_3 \psi) \right) + \partial_2 \left(\frac{h_1}{h_2 h_3} \partial_2 (h_3 \psi) \right) \right). \tag{3.11}$$

Denote by $\omega = -\mathscr{L}\psi$, the vorticity component in the symmetry direction, it follows similarly that

$$\boldsymbol{\omega} = (0,0,\omega) + \nabla \times (0,0,u). \tag{3.12}$$

At this point, we would like to introduce the following identity:

$$\mathscr{L}\psi = \nabla^2\psi - V\psi, \tag{3.13}$$

where ∇^2 is the standard Laplacian in D:

$$\nabla^2\psi = \frac{1}{h_1h_2h_3}\left(\partial_1\left(\frac{h_2h_3}{h_1}\partial_1\psi\right) + \partial_2\left(\frac{h_1h_3}{h_2}\partial_2\psi\right)\right) = \nabla\cdot\nabla\psi \tag{3.14}$$

and V is the geometric source term

$$V = \frac{-1}{h_1h_2}\left(\partial_1\left(\frac{h_2}{h_1h_3}\partial_1h_3\right) + \partial_2\left(\frac{h_1}{h_2h_3}\partial_2h_3\right)\right) = h_3\nabla^2\left(\frac{1}{h_3}\right). \tag{3.15}$$

The identity (3.13) plays an important role in the treatment of the pole singularity in our finite difference spatial discretization (5.3). In the axisymmetric case, $h_3 = 0$ on the axis of symmetry. This poses a difficulty as we discretize $\mathscr{L}$ directly using (3.11). This difficulty disappears with the equivalent operator $\nabla^2 - V$ provided $r = 0$ is not a grid point. See Section 5 for details.

The most crucial observation in this paper is that all the nonlinear terms can be written as Jacobians:

$$\begin{aligned}\boldsymbol{\omega}\times\boldsymbol{u} &= \begin{vmatrix} \boldsymbol{e}_1 & \boldsymbol{e}_2 & \boldsymbol{e}_3 \\ \frac{1}{h_3}\frac{\partial_2(h_3u)}{h_2} & -\frac{1}{h_3}\frac{\partial_1(h_3u)}{h_1} & \omega \\ \frac{1}{h_3}\frac{\partial_2(h_3\psi)}{h_2} & -\frac{1}{h_3}\frac{\partial_1(h_3\psi)}{h_1} & u \end{vmatrix} \\ &= \left(\frac{\omega}{h_3}\frac{\partial_1(h_3\psi)}{h_1} - \frac{u}{h_3}\frac{\partial_1(h_3u)}{h_1}, \frac{\omega}{h_3}\frac{\partial_2(h_3\psi)}{h_2} - \frac{u}{h_3}\frac{\partial_2(h_3u)}{h_2}, \frac{1}{h_3^2}\left(\frac{\partial_2(h_3\psi)}{h_2}\frac{\partial_1(h_3u)}{h_1} - \frac{\partial_2(h_3\psi)}{h_1}\frac{\partial_2(h_3u)}{h_2}\right)\right),\end{aligned}$$

therefore

$$(\boldsymbol{\omega}\times\boldsymbol{u})_3 = \frac{1}{h_3^2}\frac{1}{h_1h_2}J(h_3u, h_3\psi) \tag{3.16}$$

and

$$\begin{aligned}(\nabla\times(\boldsymbol{\omega}\times\boldsymbol{u}))_3 &= \frac{1}{h_1h_2}\begin{vmatrix} \partial_1 & \partial_2 \\ \frac{\omega\partial_1(h_3\psi)}{h_3} - \frac{u\partial_1(h_3u)}{h_3} & \frac{\omega\partial_2(h_3\psi)}{h_3} - \frac{u\partial_2(h_3u)}{h_3} \end{vmatrix} \\ &= \frac{1}{h_1h_2}\left(\partial_1\left(\frac{\omega}{h_3}\right)\partial_2(h_3\psi) - \partial_2\left(\frac{\omega}{h_3}\right)\partial_1(h_3\psi) - \partial_1\left(\frac{u}{h_3}\right)\partial_2(h_3\psi) + \partial_2\left(\frac{u}{h_3}\right)\partial_1(h_3u)\right) \\ &= \frac{1}{h_1h_2}J\left(\frac{\omega}{h_3}, h_3\psi\right) - \frac{1}{h_1h_2}J\left(\frac{u}{h_3}, h_3u\right).\end{aligned}$$

We therefore have the (ψ, u, ω) formulation for the 3D symmetric Navier–Stokes equation,

$$\begin{aligned}&\partial_t u + \frac{1}{h_3^2}\frac{1}{h_1h_2}J(h_3u, h_3\psi) = \nu(\nabla^2 - V)u, \\ &\partial_t\omega + \frac{1}{h_1h_2}J\left(\frac{\omega}{h_3}, h_3\psi\right) = \nu(\nabla^2 - V)\omega + \frac{1}{h_1h_2}J\left(\frac{u}{h_3}, h_3u\right), \\ &\omega = -(\nabla^2 - V)\psi,\end{aligned} \tag{3.17}$$

with the no-slip boundary condition (2.2) expressed in terms of u and ψ:

$$\boldsymbol{u}\cdot\boldsymbol{n}=\partial_\tau(h_3\psi)=0,\quad \boldsymbol{u}\cdot\boldsymbol{\tau}=\partial_n(h_3\psi)=0,\quad \boldsymbol{u}\cdot\boldsymbol{e}_3=u=0,$$

where $\boldsymbol{n}$ is the outer normal at $\partial\Omega$ and $\boldsymbol{\tau}=\boldsymbol{n}\times\boldsymbol{e}_3$. When the cross section Ω is simply connected, the no-slip boundary condition further reduces to

$$u=0,\quad \psi=0,\quad \partial_n(h_3\psi)=0\quad \text{on } \partial\Omega. \tag{3.18}$$

Next we reformulate the energy and helicity identities (2.10) and (2.11) in terms of the active variables u and ω. We first define the weighted L^2 and H^1 inner products:

$$\langle f,g\rangle=\int_\Omega h_1h_2h_3f(y_1,y_2)g(y_1,y_2)\,\mathrm{d}y_1\,\mathrm{d}y_2, \tag{3.19}$$

$$\langle \boldsymbol{f},\boldsymbol{g}\rangle=\int_\Omega h_1h_2h_3\boldsymbol{f}(y_1,y_2)\cdot\boldsymbol{g}(y_1,y_2)\,\mathrm{d}y_1\,\mathrm{d}y_2 \tag{3.20}$$

and

$$[f,g]=\left\langle\frac{1}{h_1}\partial_1 f,\frac{1}{h_1}\partial_1 g\right\rangle+\left\langle\frac{1}{h_2}\partial_2 f,\frac{1}{h_2}\partial_2 g\right\rangle+\langle f,Vg\rangle. \tag{3.21}$$

It is worth noting that

$$\langle f,(-\nabla^2+V)g\rangle=[f,g] \tag{3.22}$$

provided either $f=0$ or $\partial_n g=0$ on $\partial\Omega$.

Since $\boldsymbol{u}$ and h_i are independent of y_3, it suffice to consider the energy and helicity identities on the cross section Ω:

$$\begin{aligned}\int_\Omega|\boldsymbol{u}|^2h_1h_2h_3\,\mathrm{d}y_1\,\mathrm{d}y_2&=\langle(0,0,u)+\nabla\times(0,0,\psi),(0,0,u)+\nabla\times(0,0,\psi)\rangle\\&=\langle(0,0,u),(0,0,u)\rangle+\langle\nabla\times(0,0,\psi),\nabla\times(0,0,\psi)\rangle=\langle u,u\rangle+[\psi,\psi],\end{aligned} \tag{3.23}$$

where in the last equality, we have used (3.10), (3.13) and (3.22) and the fact that

$$\langle\nabla\times(0,0,f),\nabla\times(0,0,g)\rangle=\langle(0,0,f),\nabla\times\nabla\times(0,0,g)\rangle \tag{3.24}$$

provided either $f=0$ or $\partial_n(h_3g)=0$ on $\partial\Omega$.

Similarly, we can write

$$\int_\Omega|\boldsymbol{\omega}|^2h_1h_2h_3\,\mathrm{d}y_1\,\mathrm{d}y_2=[u,u]+\langle\omega,\omega\rangle \tag{3.25}$$

$$\begin{aligned}\int_\Omega\boldsymbol{u}\cdot\boldsymbol{\omega}h_1h_2h_3\,\mathrm{d}y_1\,\mathrm{d}y_2&=\langle(0,0,u)+\nabla\times(0,0,\psi),(0,0,\omega)+\nabla\times(0,0,u)\rangle\\&=\langle(0,0,u),(0,0,\omega)\rangle+\langle\nabla\times(0,0,\psi),\nabla\times(0,0,u)\rangle\\&=\langle(0,0,\omega),(0,0,u)\rangle.\end{aligned} \tag{3.26}$$

Therefore

$$\int_\Omega\boldsymbol{u}\cdot\boldsymbol{\omega}h_1h_2h_3\,\mathrm{d}y_1\,\mathrm{d}y_2=2\langle u,\omega\rangle \tag{3.27}$$

and

$$\int_D \boldsymbol{\omega}\cdot(\nabla\times\boldsymbol{\omega}) = \langle(0,0,\omega)+\nabla\times(0,0,u),(0,0,-(\nabla^2-V)u)+\nabla\times(0,0,\omega)\rangle$$
$$= [u,\omega]-\langle\omega,(\nabla^2-V)u\rangle, \tag{3.28}$$

we conclude with the energy and helicity identity in terms of u and ω:

$$\frac{\mathrm{d}}{\mathrm{d}t}\frac{1}{2}(\langle u,u\rangle+[\psi,\psi])+\nu([u,u]+\langle\omega,\omega\rangle)=0, \tag{3.29}$$

$$\frac{\mathrm{d}}{\mathrm{d}t}\langle u,\omega\rangle+\nu([u,\omega]-\langle\omega,(\nabla^2-V)u\rangle)=0. \tag{3.30}$$

For MHD flows with coordinate symmetry, we can similarly write

$$\begin{aligned}
&\boldsymbol{u}=(0,0,u)+\nabla\times(0,0,\psi),\\
&\boldsymbol{\omega}=(0,0,\omega)+\nabla\times(0,0,u),\quad \omega=-(\nabla^2-V)\psi,\\
&\boldsymbol{b}=(0,0,b)+\nabla\times(0,0,a),\\
&\boldsymbol{j}=(0,0,\jmath)+\nabla\times(0,0,b),\quad \jmath=-(\nabla^2-V)a,
\end{aligned} \tag{3.31}$$

and reformulate all the nonlinear terms as Jacobians:

$$\begin{aligned}
&(\boldsymbol{\omega}\times\boldsymbol{u})_3=\frac{1}{h_3^2}\frac{1}{h_1h_2}J(h_3u,h_3\psi),\\
&(\boldsymbol{j}\times\boldsymbol{b})_3=\frac{1}{h_3^2}\frac{1}{h_1h_2}J(h_3b,h_3a),\\
&(\boldsymbol{u}\times\boldsymbol{b})_3=\frac{1}{h_3^2}\frac{1}{h_1h_2}J(h_3\psi,h_3a),
\end{aligned} \tag{3.32}$$

$$\begin{aligned}
&(\nabla\times(\boldsymbol{\omega}\times\boldsymbol{u}))_3=\frac{1}{h_1h_2}J\left(\frac{\omega}{h_3},h_3\psi\right)-\frac{1}{h_1h_2}J\left(\frac{u}{h_3},h_3u\right),\\
&(\nabla\times(\boldsymbol{j}\times\boldsymbol{b}))_3=\frac{1}{h_1h_2}J\left(\frac{\jmath}{h_3},h_3a\right)-\frac{1}{h_1h_2}J\left(\frac{b}{h_3},h_3b\right),\\
&(\nabla\times(\boldsymbol{u}\times\boldsymbol{b}))_3=\frac{1}{h_1h_2}J\left(\frac{u}{h_3},h_3a\right)-\frac{1}{h_1h_2}J\left(\frac{b}{h_3},h_3\psi\right),
\end{aligned} \tag{3.33}$$

and the 3D symmetric MHD takes the form:

$$\partial_t u+\frac{1}{h_3^2}\frac{1}{h_1h_2}J(h_3u,h_3\psi)=\nu(\nabla^2-V)u+\frac{\alpha}{h_3^2}\frac{1}{h_1h_2}J(h_3b,h_3a),$$

$$\partial_t\omega+\frac{1}{h_1h_2}J\left(\frac{\omega}{h_3},h_3\psi\right)-\frac{1}{h_1h_2}J\left(\frac{u}{h_3},h_3u\right)=\nu(\nabla^2-V)\omega+\frac{\alpha}{h_1h_2}J\left(\frac{\jmath}{h_3},h_3a\right)-\frac{\alpha}{h_1h_2}J\left(\frac{b}{h_3},h_3b\right),$$

$$\omega=-(\nabla^2-V)\psi,$$

$$\partial_t a = \eta(\nabla^2 - V)a + \frac{1}{h_3^2}\frac{1}{h_1 h_2} J(h_3\psi, h_3 a),$$

$$\partial_t b = \eta(\nabla^2 - V)b + \frac{1}{h_1 h_2} J\left(\frac{u}{h_3}, h_3 a\right) - \frac{1}{h_1 h_2} J\left(\frac{b}{h_3}, h_3\psi\right),$$

$$\jmath = -(\nabla^2 - V)a. \tag{3.34}$$

On a simply connected Ω, the perfectly conducting wall conditions $\boldsymbol{j} \times \boldsymbol{n} = \boldsymbol{0}$ is given by

$$\jmath = 0, \quad \partial_n(h_3 b) = 0 \quad \text{on } \partial\Omega. \tag{3.35}$$

Since a is a computational variable, it is convenient to take the alternative form of $\jmath = 0$ in terms of a. In view of (3.18) and the fourth equation in (3.34), the boundary condition for a is simply given by $\partial_t a = 0$. Therefore we have the boundary condition for the symmetric MHD:

$$u = 0, \quad \psi = 0, \quad \partial_n(h_3\psi) = 0, \quad \partial_t a = 0, \quad \partial_n(h_3 b) = 0 \quad \text{on } \partial\Omega. \tag{3.36}$$

This is also consistent with the boundary constraint $\partial_t(\boldsymbol{b} \cdot \boldsymbol{n}) = 0$, a direct consequence of the Faraday equation.

In the next section, we will develop energy and helicity preserving numerical schemes for the vorticity-stream formulation of symmetric Navier–Stokes and MHD equations. We will give detail derivation for the Navier–Stokes equation (3.17) only. Generalization to the MHD equation (3.34) is straight forward. The energy and helicity identities for the MHD equation formulated in terms of u, ω, a and b are given in the Appendix A.

4. Energy and helicity preserving schemes

4.1. The permutation identity and conservation laws revisited

We first derive the permutation identity associated with the Jacobians. Observe that

$$J(a,b) = \nabla a \cdot \nabla^\perp b = \frac{1}{3}\big(\nabla a \cdot \nabla^\perp b + \nabla \cdot (a\nabla^\perp b) + \nabla^\perp \cdot (b\nabla a)\big), \tag{4.1}$$

and define the following trilinear form:

$$T(a,b,c) = \frac{1}{3}\int_\Omega \big(c(\nabla a \cdot \nabla^\perp b) + a(\nabla b \cdot \nabla^\perp c) + b(\nabla c \cdot \nabla^\perp a)\big). \tag{4.2}$$

It follows that

$$\int_\Omega cJ(a,b) = T(a,b,c) - \int_{\partial\Omega} c(a\partial_\tau b - b\partial_\tau a), \tag{4.3}$$

and we have the following

Proposition 1. *Let a, b, c be smooth functions defined on Ω with $c(a\partial_\tau b - b\partial_\tau a) = 0$ on $\partial\Omega$. Then*

$$\int_\Omega cJ(a,b) = T(a,b,c). \tag{4.4}$$

The assumption in Proposition 1 is valid on the physical boundary provided at least one of a, b or c contains either ψ or u as a factor. This is the case for all the Jacobians in (3.17). It is also valid on the axis of rotation for axisymmetric flows as all the dependent variables are the swirling components of axisymmetric vector fields and satisfy odd extension across the axis of rotation. See also (5.4).

From (4.2), we can easily derive the following permutation identity which plays an essential role in our development of energy and helicity preserving schemes:

$$T(a,b,c) = T(b,c,a) = T(c,a,b), \qquad T(a,b,c) = -T(b,a,c). \tag{4.5}$$

Indeed, we can give an alternative (and much simpler) derivation of (3.29) and (3.30) using (4.5). We take the weighted inner product (3.19) of the first equation in (3.17) with υ, the second with φ to get

$$\begin{aligned} &\langle \upsilon, \partial_t u\rangle + T(h_3 u, h_3\psi, \upsilon/h_3) = \nu\langle \upsilon, (\nabla^2 - V)u\rangle,\\ &[\varphi, \partial_t\psi] + T(\omega/h_3, h_3\psi, h_3\varphi) = \nu\langle \varphi, (\nabla^2 - V)\omega\rangle + T(u/h_3, h_3 u, h_3\varphi). \end{aligned} \tag{4.6}$$

The energy and helicity identities (3.29) and (3.30) follow easily from the permutation identity (4.5) by taking $(\upsilon,\varphi) = (u,\psi)$ and (ω,u) in (4.6) respectively.

In view of (4.6), it is clear that in order to preserve the energy and helicity identities numerically, it suffices to discretize the Jacobians in such a way that the discrete analogue of the permutation identity (4.5) is satisfied. In the next subsection, we will show how this can be done for a second order scheme based on standard centered differencing. This principle can be generalized to higher order finite difference, finite element and spectral Galerkin methods. See also Remark (2) in Section 4.2.

4.2. Finite difference method and discrete permutation identities

With the standard notation,

$$D_1 f(y_1,y_2) = \frac{f(y_1+\Delta y_1/2, y_2) - f(y_1-\Delta y_1/2, y_2)}{\Delta y_1}, \tag{4.7}$$

$$\tilde{D}_1 f(y_1,y_2) = \frac{f(y_1+\Delta y_1, y_2) - f(y_1-\Delta y_1, y_2)}{2\Delta y_1}, \tag{4.8}$$

$$\tilde{\nabla}_h = (\tilde{D}_1, \tilde{D}_2), \quad \tilde{\nabla}_h^{\perp} = (-\tilde{D}_2, \tilde{D}_1), \tag{4.9}$$

the finite difference approximation of ∇^2 and the Jacobians are given by

$$\nabla_h^2 f = \frac{1}{h_1 h_2 h_3}\left(D_1\left(\frac{h_2 h_3}{h_1} D_1 f\right) + D_2\left(\frac{h_1 h_3}{h_2} D_2 f\right)\right) \tag{4.10}$$

and

$$J_h(f,g) = \frac{1}{3}\left(\tilde{\nabla}_h f \cdot \tilde{\nabla}_h^{\perp} g + \tilde{\nabla}_h \cdot (f\,\tilde{\nabla}_h^{\perp} g) + \tilde{\nabla}_h^{\perp} \cdot (g\tilde{\nabla}_h f)\right). \tag{4.11}$$

Altogether, the finite difference approximation of Navier–Stokes equation is given by

$$\partial_t u + \frac{1}{h_3^2}\frac{1}{h_1 h_2} J_h(h_3 u, h_3 \psi) = \nu(\nabla_h^2 - V)u,$$

$$\partial_t \omega + \frac{1}{h_1 h_2} J_h\left(\frac{\omega}{h_3}, h_3\psi\right) = \nu(\nabla_h^2 - V)\omega + \frac{1}{h_1 h_2} J_h\left(\frac{u}{h_3}, h_3 u\right), \tag{4.12}$$

$$\omega = (-\nabla_h^2 + V)\psi.$$

From (4.11), we will show that

$$\Delta y_1 \Delta y_2 \sum_{i,j} c_{i,j} J_h(a,b)_{i,j} = \Delta y_1 \Delta y_2 \frac{1}{3} \sum_{i,j} \left(c\tilde{\nabla}_h a \cdot \tilde{\nabla}_h^{\perp} b + a\tilde{\nabla}_h b \cdot \tilde{\nabla}_h^{\perp} c + b\tilde{\nabla}_h c \cdot \tilde{\nabla}_h^{\perp} a \right)_{i,j}. \tag{4.13}$$

Therefore, if we define $T_h(a,b,c)$ as the right hand side of (4.13), we recover the discrete permutation identity

$$T_h(a,b,c) = T_h(b,c,a) = T_h(c,a,b), \qquad T_h(a,b,c) = -T_h(b,a,c). \tag{4.14}$$

To see this, we first look at the quasi-2D flows where $\Omega = R^2$ or T^2 and the physical boundary is not present. We begin with the following identity:

$$\sum_{j=1}^{N-1} f_j(g_{j+1} - g_{j-1}) = -\sum_{j=1}^{N-1} (f_{j+1} - f_{j-1}) g_j + f_{N-1} g_N + f_N g_{N-1} - f_0 g_1 - f_1 g_0, \tag{4.15}$$

ignoring the boundary terms, we can simply write (4.15) as

$$\sum_j f_j(g_{j+1} - g_{j-1}) = -\sum_j (f_{j+1} - f_{j-1}) g_j \tag{4.16}$$

and consequently

$$\Delta y_1 \Delta y_2 \sum_j \sum_i c\tilde{\nabla}_h \cdot (a\tilde{\nabla}_h^{\perp} b) = -\Delta y_1 \Delta y_2 \sum_{i,j} a\tilde{\nabla}_h c \cdot \tilde{\nabla}_h^{\perp} b, \tag{4.17}$$

$$\Delta y_1 \Delta y_2 \sum_i \sum_j c\tilde{\nabla}_h^{\perp} \cdot (b\tilde{\nabla}_h a) = -\Delta y_1 \Delta y_2 \sum_{i,j} b\tilde{\nabla}_h^{\perp} c \cdot \tilde{\nabla}_h a, \tag{4.18}$$

and (4.13) follows.

As to the viscous terms, we denote the discrete weighted inner products by

$$\langle \phi, \psi \rangle_h = \sum_{i,j} (h_1 h_2 h_3 \phi\psi)_{i,j} \Delta y_1 \Delta y_2, \tag{4.19}$$

$$[\phi, \psi]_h = \sum_{i,j} \left(\frac{h_2 h_3}{h_1} (D_1\phi)(D_1\psi) \right)_{i-1/2,j} \Delta y_1 \Delta y_2 + \sum_{i,j} \left(\frac{h_1 h_3}{h_2} (D_2\phi)(D_2\psi) \right)_{i,j-1/2} \Delta y_1 \Delta y_2 + \langle \phi, V\psi \rangle_h. \tag{4.20}$$

It is easy to see that

$$\langle \phi, (\nabla_h^2 - V)\psi \rangle_h = -[\phi, \psi]_h, \tag{4.21}$$

when there is no boundary terms involved.

The discrete energy and helicity identities is a direct consequence of (4.13) and (4.21). Take the discrete weighted inner product (4.19) of the first equation in (4.12) with υ, the second with φ, it follows that

$$\begin{aligned}&\langle \upsilon, \partial_t u\rangle_h + T_h(h_3 u, h_3\psi, \upsilon/h_3) = \nu\langle \upsilon, (\nabla_h^2 - V)u\rangle_h,\\ &[\varphi, \partial_t\psi]_h + T_h(\omega/h_3, h_3\psi, h_3\varphi) = \nu\langle \varphi, (\nabla_h^2 - V)\omega\rangle_h + T_h(u/h_3, h_3 u, h_3\varphi),\end{aligned} \tag{4.22}$$

and we get the discrete energy identity

$$\frac{\mathrm{d}}{\mathrm{d}t}\frac{1}{2}(\langle u, u\rangle_h + [\psi, \psi]_h) + \nu([u, u]_h + \langle \omega, \omega\rangle_h) = 0 \tag{4.23}$$

by taking $\upsilon = u$, $\varphi = \psi$ in (4.22). Also the discrete helicity identity

$$\frac{\mathrm{d}}{\mathrm{d}t}\langle u, \omega\rangle_h + \nu([u, \omega]_h - \langle \omega, (\nabla_h^2 - V)u\rangle_h) = 0 \tag{4.24}$$

follows by taking $\upsilon = \omega$, $\varphi = u$.

In the next section, we will focus on axisymmetric flows and show that both (4.13) and (4.21) remain valid in the presence of the pole singularity and physical boundary. As a consequence, (4.23) and (4.24) follow as well.

Remarks.

(1) In the 2D case, the approximation $J_h(a, b)$ is equivalent to the classical Arakawa scheme [1].

(2) The energy and helicity preserving scheme (4.12) can be generalized to higher order finite difference scheme by replacing $\tilde{\nabla}_h$ and ∇_h with higher order centered difference approximations of ∇. The discrete analogue of the permutation identity (4.5) remains valid. Similarly, to maintain the energy and helicity preserving property in finite element and spectral Galerkin approximations, it suffices to define $J_h(a, b)$ through its pairing with test function c by

$$\langle c, J_h(a, b)\rangle \equiv T(a, b, c).$$

5. Finite difference scheme for axisymmetric flows

An important class of flows with symmetry is the axisymmetric ones. In this section, we give more details of the finite difference EHPS applied to axisymmetric flows, including the treatment of the pole singularity and physical boundary conditions.

For axisymmetric flows, the cylindrical coordinate system $(y_1, y_2, y_3) = (x, r, \theta)$ with $r^2 = y^2 + z^2$ and $\theta = \arctan(z/y)$ results in $(h_1, h_2, h_3) = (1, 1, r)$ and the Navier–Stokes equation can be written as

$$\begin{aligned}&u_t + \frac{1}{r^2}J(ru, r\psi) = \nu\left(\nabla^2 - \frac{1}{r^2}\right)u,\\ &\omega_t + J\left(\frac{\omega}{r}, r\psi\right) = \nu\left(\nabla^2 - \frac{1}{r^2}\right)\omega + J\left(\frac{u}{r}, ru\right),\\ &\omega = \left(-\nabla^2 + \frac{1}{r^2}\right)\psi.\end{aligned} \tag{5.1}$$

In [2], it is shown that the only possible singularity for axisymmetric flow of Navier–Stokes equation is on the axis. We therefore may want to refine the grids locally near the axis. This can be done by a simple change of variables. For example, take

$$(y_1, y_2, y_3) = (x, s, \theta),$$

with $s = r^{1/2} = (y^2 + z^2)^{1/4}$. This gives $(h_1, h_2, h_3) = (1, 2s, s^2)$ and the Navier–Stokes equation reads

$$\begin{aligned} &u_t + \frac{1}{2s^5} J\left(s^2 u, s^2 \psi\right) = \nu\left(\nabla^2 - \frac{1}{s^4}\right) u, \\ &\omega_t + \frac{1}{2s} J\left(\frac{\omega}{s^2}, s^2 \psi\right) = \nu\left(\nabla^2 - \frac{1}{s^4}\right) \omega + \frac{1}{2s} J\left(\frac{u}{s^2}, s^2 u\right), \\ &\omega = \left(-\nabla^2 + \frac{1}{s^4}\right) \psi. \end{aligned} \tag{5.2}$$

5.1. Cylindrical coordinate system and the pole singularity

In either (5.1) or (5.2), the Navier–Stokes equation exhibits coordinate singularity $1/r$ ($1/s$, respectively) at the axis of rotation. A simple and effective treatment for finite difference scheme is to shift the grids half grid size off the axis [12]:

$$y_2(j) = \left(j - \frac{1}{2}\right) \Delta y_2, \quad j = 0, 1, 2, \ldots \tag{5.3}$$

That is, $r_j = (j - \frac{1}{2})\Delta r$, $j = 0, 1, 2, \ldots$ in (x, r, θ) coordinates and $s_j = (j - \frac{1}{2})\Delta s$, $j = 0, 1, 2, \ldots$ in (x, s, θ) coordinates.

Since u, ψ, ω are the swirling components of $\boldsymbol{u}, \boldsymbol{\psi}, \boldsymbol{\omega}$, they satisfy the reflection boundary condition, or in other words, odd extension across the axis of rotation:

$$u(i, 0) = -u(i, 1), \quad \psi(i, 0) = -\psi(i, 1), \quad \omega(i, 0) = -\omega(i, 1) \tag{5.4}$$

and

$$h_1(0, j) = h_1(1, j), \quad h_2(0, j) = h_2(1, j), \quad h_3(0, j) = h_3(1, j) \tag{5.5}$$

for the local stretching factors.

If we denote by j the index in the direction parallel to the axis, it follows from (4.15) that

$$\sum_{j=1}^{\infty} f_j (g_{j+1} - g_{j-1}) = -\sum_{j=1}^{\infty} g_j (f_{j+1} - f_{j-1}) - (f_0 g_1 + g_0 f_1). \tag{5.6}$$

When we repeat the procedure outlined in (4.13)–(4.16) there is an additional boundary contribution at the pole:

$$\sum_i (f_{i,0} g_{i,1} + g_{i,0} f_{i,1}),$$

where $f = c$ and $g = b\tilde{D}_x a - a\tilde{D}_x b$ (see also (A.19)).

In view of the reflection boundary condition (5.4), we have

$$f_{i,0} = -f_{i,1}, \quad g_{i,0} = g_{i,1}. \tag{5.7}$$

The boundary contribution at the pole cancels exactly and the discrete permutation identity (4.14) remains valid even in the presence of the pole singularity.

As to the viscous terms, it is easy to see that (4.21) remains valid across the axis since $r_{1/2} = s_{1/2} = 0$ and

$$\sum_{j=1}^{\infty} f_j(g_{j+1/2} - g_{j-1/2}) = -\left(\frac{1}{2}(f_1 - f_0)g_{1/2} + \sum_{j=2}^{\infty}(f_j - f_{j-1})g_{j-1/2}\right) - \frac{1}{2}(f_1 + f_0)g_{1/2}. \tag{5.8}$$

This also explains why we choose to discretize $\nabla^2 - V$ instead of $\mathscr{L}$ in (4.12).

In summary, the discrete energy and helicity identity (4.23) and (4.24) remain valid for axisymmetric flows in the whole space.

5.2. Treatment of physical boundary conditions

In order to preserve the conservation laws for the energy and helicity in the presence of the physical boundary, the no-slip boundary condition needs to be realized in a proper way. We consider the flow confined in a cylinder $\{x_{\min} < x < x_{\max}, 0 < r < r_{\max}\}$, and let i be the index in the axial direction. Similar to (4.15), we have

$$\sum_{i=1}^{M-1} f_i(g_{i+1} - g_{i-1}) = -\sum_{i=1}^{M-1}(f_{i+1} - f_{i-1})g_i + f_{M-1}g_M + f_M g_{M-1} - f_0 g_1 - f_1 g_0, \tag{5.9}$$

it follows that if we place the physical boundary in the middle of grid points

$$x_{\frac{1}{2}} = x_{\min}, \ldots, x_{M-\frac{1}{2}} = x_{\max}, \qquad r_{\frac{1}{2}} = 0, \ldots, r_{N-\frac{1}{2}} = r_{\max} \tag{5.10}$$

a second order approximation for two of the no-slip boundary condition $\psi = \partial_n \psi = 0$ is realized by simply imposing

$$\psi_{0,j} = \psi_{1,j} = 0, \quad \psi_{M-1,j} = \psi_{M,j} = 0, \quad \psi_{i,N-1} = \psi_{i,N} = 0. \tag{5.11}$$

Table 1
Errors and orders of accuracy for example 1

	Mesh	L^2 error	Order	L^∞ error	Order
ψ	50×64	1.6373E−3	–	1.4779E−3	–
	100×128	4.1033E−4	1.997	3.7036E−4	1.997
	200×256	1.0289E−4	1.996	9.2885E−5	1.995
	400×512	2.5770E−5	1.997	2.3259E−5	1.998
	800×1024	6.4488E−6	1.999	5.8198E−6	1.999
u	50×64	1.2637E−2	–	3.8124E−2	–
	100×128	2.8318E−3	2.158	7.9906E−3	2.254
	200×256	6.7669E−4	2.065	1.9580E−3	2.029
	400×512	1.6720E−4	2.017	4.8754E−4	2.006
	800×1024	4.1679E−5	2.004	1.2146E−4	2.005
ω	50×64	2.3133E−2	–	4.0879E−2	–
	100×128	5.7070E−3	2.019	9.3925E−3	2.122
	200×256	1.4162E−3	2.011	2.2181E−3	2.082
	400×512	3.5390E−4	2.001	6.3534E−4	1.804
	800×1024	8.8512E−5	1.999	1.6974E−4	1.904

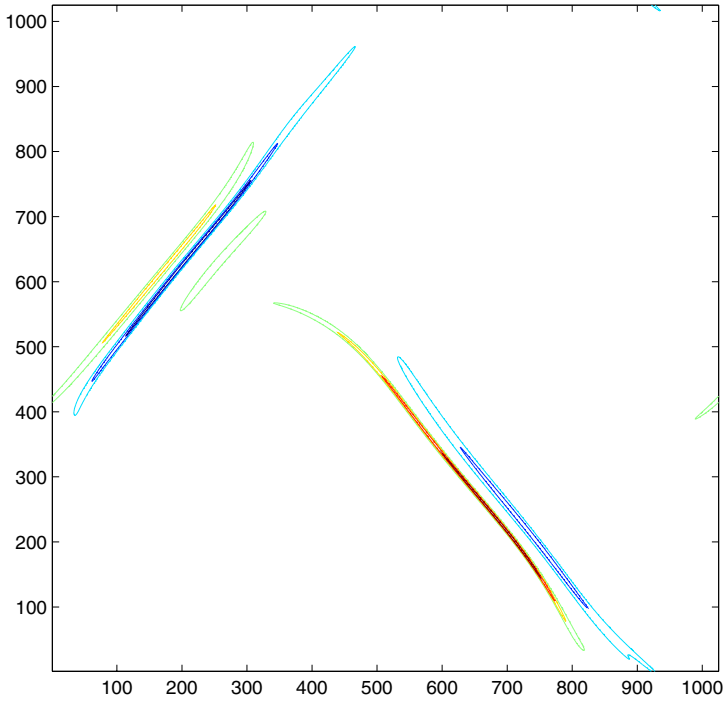

Fig. 1. Example 2, contour plot of the current density j at $t = 2.7$.

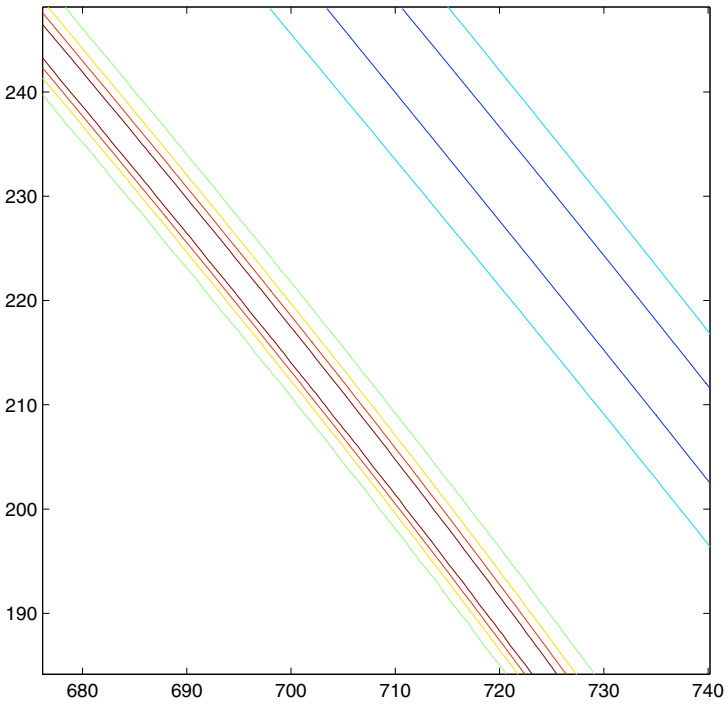

Fig. 2. Example 2, close up of Fig. 1. The current sheet is resolved with about 8 grid points.

Also, a second order approximation of the third no slip condition $u = 0$ is given by

$$u_{0,j} + u_{1,j} = 0, \quad u_{M-1,j} + u_{M,j} = 0, \quad u_{i,N-1} + u_{i,N} = 0. \tag{5.12}$$

We can show that under (5.11) and (5.12), the discrete permutation identity (4.14) are indeed verified and the energy and helicity identities (4.23) and (4.24) remain valid. The details are given in the Appendix A.

In the case of MHD equation, the discrete counterpart of the boundary term in (4.3) does not drop out automatically. A simple remedy is to add a correction term to the Jacobians at points $(1, j)$, $(M-1, j)$ and $(i, N-1)$. Since these points are $O(\Delta x)$ and $O(\Delta r)$ from the boundary, this correction is of $O(\Delta x^2 + \Delta r^2)$ and the resulting scheme is still second order consistent with the equation. This approach is quite artificial so we will not pursue further.

We are unable to find a simple and local numerical boundary condition that preserves the MHD energy and helicity identities in the presence of physical boundaries.

In practice, a more convenient way of realizing (3.36) is to place the grid points on the physical boundary as is usually done (the pole $r = 0$ is still located at $j = \frac{1}{2}$). In other words, we put

$$x_0 = x_{\min}, \ldots, x_M = x_{\max}, \qquad r_{\frac{1}{2}} = 0, \ldots, r_N = r_{\max}. \tag{5.13}$$

The $u = \psi = 0$ condition are given by

$$\psi_{0,j} = \psi_{M,j} = \psi_{i,N} = 0, \tag{5.14}$$

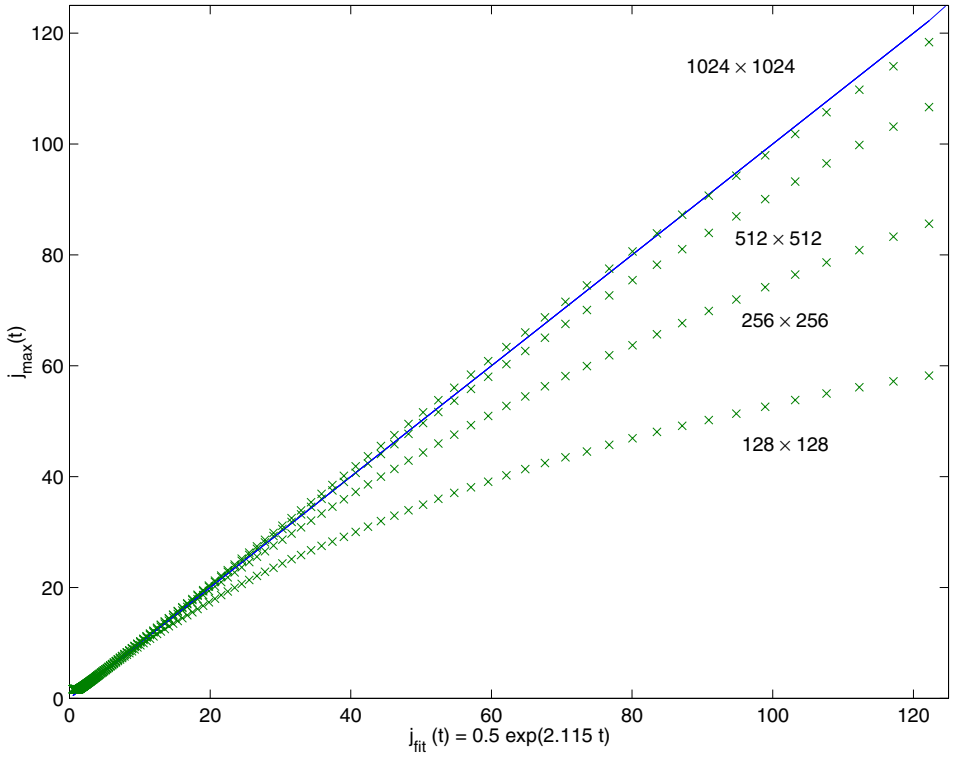

Fig. 3. Example 2, time evolution history of maximum current sheet with different resolutions. j_{fit}: data computed in [4] using equivalence of 4096^2 resolution.

$$u_{0,j} = u_{M,j} = u_{i,N} = 0, \tag{5.15}$$

The boundary condition $\partial_n(h_3\psi) = 0$, or equivalently $\partial_n\psi = 0$ since $\psi = 0$ on the boundary, can be realized as

$$\psi_{-1,j} = \psi_{1,j}, \quad \psi_{M+1,j} = \psi_{M-1,j}, \quad \psi_{i,N+1} = \psi_{i,N-1}. \tag{5.16}$$

Similarly

$$\partial_t a_{0,j} = 0, \quad \partial_t a_{M,j} = 0, \quad \partial_t a_{i,N} = 0, \tag{5.17}$$

$$(h_3 b)_{-1,j} = (h_3 b)_{1,j}, \quad (h_3 b)_{M+1,j} = (h_3 b)_{M-1,j}, \quad (h_3 b)_{i,N+1} = (h_3 b)_{i,N-1}. \tag{5.18}$$

The boundary conditions (5.16) and (5.18) uniquely determines the values of ψ and b on the ghost points $(-1, j)$, $(M + 1, j)$ and $(i, N + 1)$. The vorticity boundary condition can be easily derived from (5.16), known as Thom's formula:

$$\omega_{0,j} = \frac{2\psi_{1,j}}{(\Delta x)^2}. \tag{5.19}$$

In this setting, the active computational variables are u, ω and a at interior points and b at interior and boundary points.

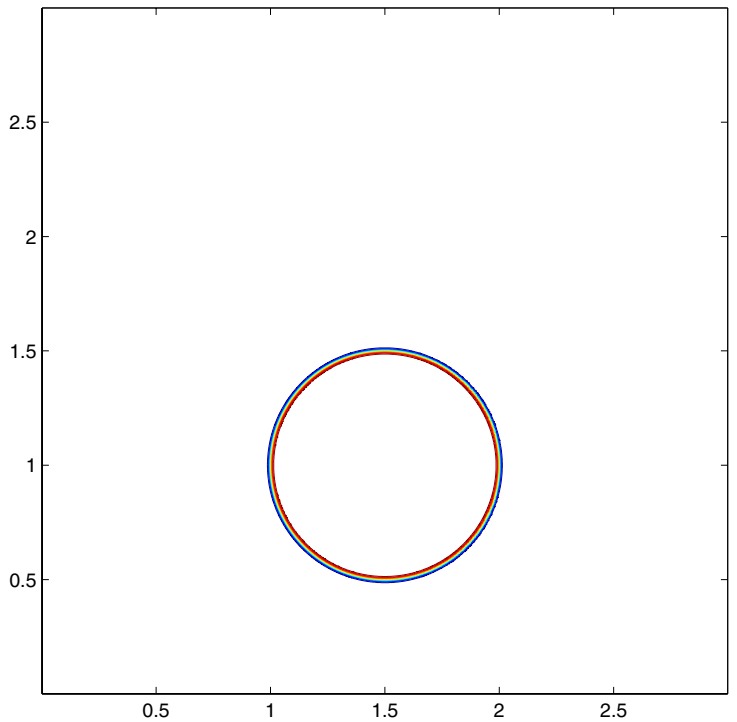

Fig. 4. Example 3, contour plot of u at $t = 0$. Horizontal axis: x, vertical axis: r.

Notice that the vorticity boundary condition for (5.10) and (5.11) corresponds to

$$\omega_{1,j} = \frac{\psi_{2,j}}{(\Delta x)^2}, \tag{5.20}$$

which differs from Thom's formula by a factor of 2. It is also known as Fromm's formula. If the grid points were placed right on the boundary as in (5.13), Fromm's formula reduces to a first order scheme, see [15]. It is indeed a second order scheme when the boundary is placed between the grid points (5.10). The second order convergence of (5.10) with (5.20) has been verified in our numerical tests. See Example 1 in Section 6.

Remarks.

(1) With a standard but somewhat lengthy truncation error analysis and a clever use of the discrete permutation identity (4.14), we can prove the following error estimate for axisymmetric flows:

$$\|u - u_h\| + \|\nabla_h(\psi - \psi_h)\|_1 \leqslant C(\Delta x^2 + \Delta r^2\sqrt{|\log \Delta r|}) \quad \text{in } x, r, \theta \text{ coordinates}$$

and

$$\|u - u_h\| + \|\nabla_h(\psi - \psi_h)\|_1 \leqslant C(\Delta x^2 + \Delta s^2) \quad \text{in } x, s, \theta \text{ coordinates},$$

where $\|f\|^2 = \langle f, f\rangle_h$ and $\|f\|_1^2 = [f, f]_h$. The details will be reported in a forthcoming paper [10].

(2) It is worth noting that this numerical conservation property is very similar to the classical Zabusky–Kruskal scheme for the KdV equation [7]:

$$u_t + uu_x + 6u_{xxx} = 0 \tag{5.21}$$

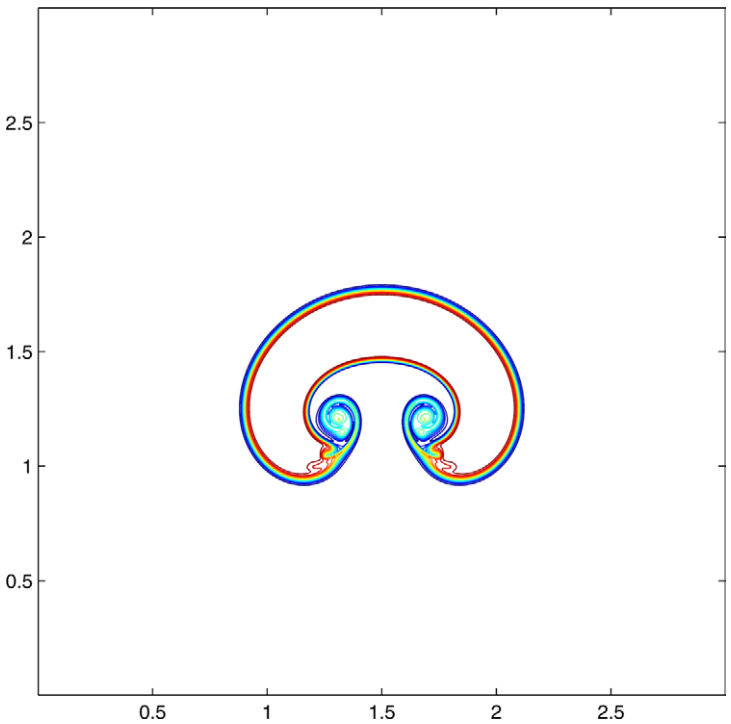

Fig. 5. Example 3, contour plot of u at $t = 2$.

in which the convection term is discretized as

$$(uu_x)_h = \frac{1}{3}u\tilde{D}_x u + \frac{2}{3}\tilde{D}_x(u^2/2) = \frac{u_{j-1}+u_j+u_{j+1}}{3}\tilde{D}_x u_j, \tag{5.22}$$

and it gives local conservation for both u_j and u_j^2.

(3) Since

$$\frac{J(a,b)}{h_1 h_2} = \frac{|\frac{\partial(a,b)}{\partial(y_1,y_2)}|}{|\frac{\partial(x_1,x_2)}{\partial(y_1,y_2)}|}, \tag{5.23}$$

it follows that the Jacobian formulation is also valid for nonorthogonal (z_1, z_2) coordinates in the (y_1, y_2) plan, as long as Ω is orthogonal to y_3. We simply replace (5.23) by

$$\frac{|\frac{\partial(a,b)}{\partial(z_1,z_2)}|}{|\frac{\partial(x_1,x_2)}{\partial(z_1,z_2)}|} = \frac{J(a,b)}{|\frac{\partial(x_1,x_2)}{\partial(z_1,z_2)}|} \tag{5.24}$$

in the (z_1, z_2, y_3) coordinates. It is therefore straight forward to generalize EHPS to non-orthogonal coordinate system to simulate flows in irregular domains using fixed or moving mesh.

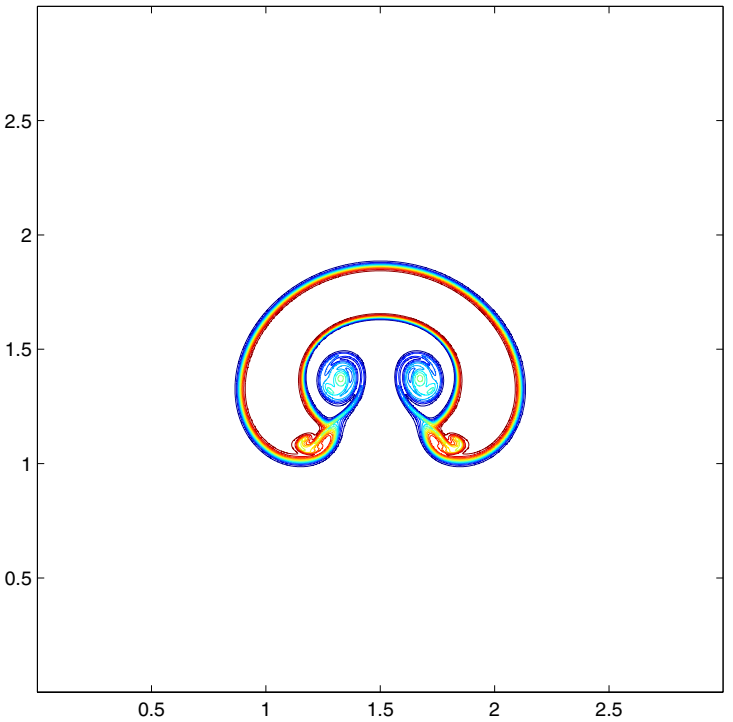

Fig. 6. Example 3, contour plot of u at $t = 2.5$.

6. Numerical examples

In the examples below, we perform numerical simulations using second order finite difference EHPS with uniform grids and classical RK4 for time integration. For axisymmetric flows, the azimuthal convection is not evolved numerically ($\partial_\theta = 0$) and therefore finite difference method is not restrictive in terms of stability constraint unless the (x, s, θ) coordinate were used. We have used fixed Δt for convenience. The CFL number varies with time and the maximal CFL number ranges from around 2.0 (Examples 1 and 2) to 2.8 (Example 3), or from 0.5 to 0.7 per Runge–Kutta step. The energy and helicity identities in Examples 2 and 3 are preserved numerically up to 9–11 digits, consistent with the truncation error in time ($\Delta t = 0.005$, $(\Delta t)^4 = O(10^{-10})$).

6.1. Example 1: accuracy check

We first check the accuracy of EHPS for axisymmetric Navier–Stokes equation. We setup the problem in a cylinder $\{0 < x < \pi, 0 < r < \pi\}$ with $\nu = 0.001$ and exact solution

$$\psi(x, r, t) = \cos(t)\sin(r)\cos(r/2)\sin^2(x), \quad u(x, r, t) = \cos(t)\sin(r)\sin(x).$$

Here $\Delta t = 0.05$ for the coarsest grid and scales with the mesh size. The result at $t = 3$ is given in Table 1. Clear second order accuracy is verified.

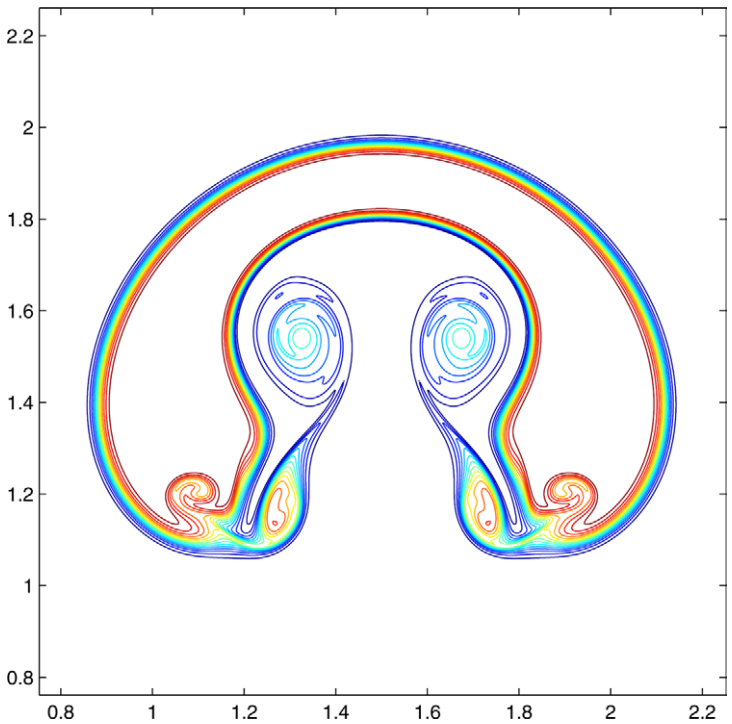

Fig. 7. Example 3, contour plot of u at $t = 3.0$.

6.2. Example 2: Orszag–Tang vortex

In this example, we repeat the calculation done by Friedel et al. [4] for ideal 2D MHD equation ($b = u = 0$ and $v = \eta = 0$ in (3.34)) using local mesh refinement technique. The underlying scheme in [4] is a second order upwind scheme combined with projection method on the primitive variable for the fluid part and potential formulation for the magnetic part. The initial data is given by

$$\psi(x, y, 0) = \cos(x + 1.4) + \cos(y + 2.0), \quad a(x, y, 0) = \tfrac{1}{3}(\cos(2x + 2.3) + \cos(y + 6.2))$$

on a 2π periodic box. This configuration typically develops singularity-like structure known as current sheets where the current density is observed to grow exponentially in time and thickness shrinks at exponential rate as well. We monitor the growth of the maximum of the current sheet during our simulation. This problem is a good test on the performance of EHPS since excessive numerical viscosity can easily smear out the current sheet. In [4], the initial resolution is 256^2 and adaptively refined on regions where the solution develops large variation. At $t = 2.7$, the finest mesh corresponds to the resolution of 4096^2 grids.

As a comparison, we repeat the same calculation with fixed resolution 1024^2 and $\Delta t = 0.005$. The contour plot of the current density j at $t = 2.7$ is shown in Fig. 1, which agrees well with the calculation done in [4]. Fig. 2 is a close up view of the same plot and we see the strong current sheet is well resolved with only 7–8 grid points across the sheet.

In addition, we plot the history of time evolution of the current sheet maximum against the simulated result $j_{\text{fit}}(t)$ reported in [4]. Compared with the same plot ([4], Fig. 3) of the fixed resolution calculation done

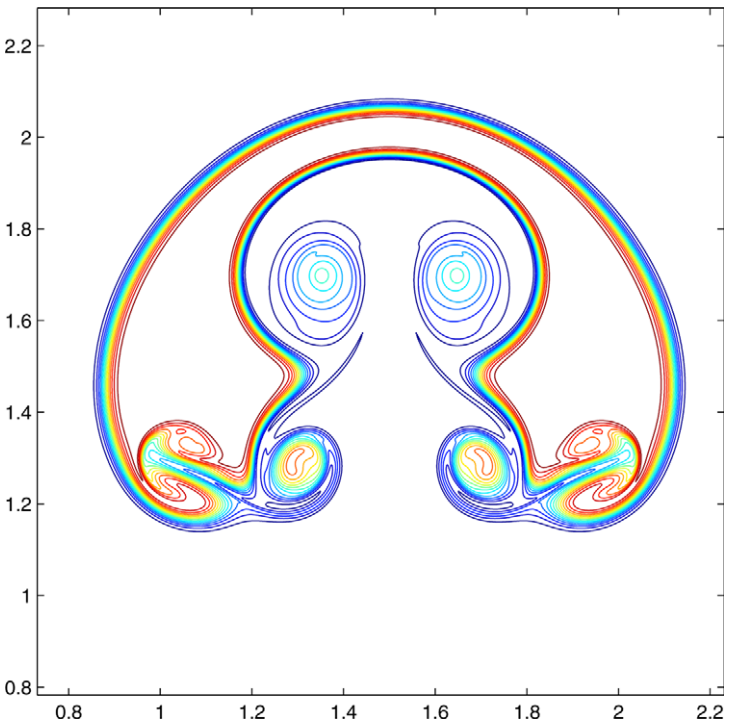

Fig. 8. Example 3, contour plot of u at $t = 3.5$.

there, we can see that EHPS is much less dissipative. Overall, we can achieve the same resolution with about half the number of grids in each space direction.

For 2D MHD, the magnetic helicity is identically zero and $\int a^2$ emerges as an additional conserved quantity. This quantity is also preserved numerically by EHPS.

6.3. Example 3: axisymmetric flow in a cylinder

We setup another test problem on a cylindrical domain $0 < x < 3$, $0 < r < 3$, with $\nu = 0.0001$ and initial data:

$$\psi(x,r,0) = 0, \quad u(x,r,0) = \frac{1}{2r}\left(1 - \tanh\left(100\left((r-1)^2 + (x-1.5)^2 - 1/4\right)\right)\right)$$

and the no-slip condition. The initial configuration corresponds to a tube of flow in a circular cross section region with uniform angular momentum and the flow outside is at rest. At $t > 0$, the flow closer to the axis is thus driven outward and generates complicated flow patterns at later time. This situation is very similar to a rising bubble in 2D Boussinesq flow. Note that this flow configuration corresponds to a strong vortex sheet at the boundary of the circular region (see Fig. 4).

The simulation is done with 1536^2 grids and $\Delta t = 0.005$. We remark here that we can afford such high resolution simulation on an ordinary desktop. This is a combined effect of the vorticity-stream formulation, explicit time integration for the nonlinear terms, and the local boundary condition that effectively decouples the Navier–Stokes equation into 2 scalar evolution equations.

Several contour plots of u are given in Figs. 4–8. The details of the complicated flow structure is well captured.

7. Conclusions

For 3D symmetric flows, we reformulated all the nonlinear terms in Navier–Stokes equation and MHD in terms of Jacobians. The physical conservation laws for energy and helicities follow directly from the permutation identity associated with the Jacobians.

We showed how to design numerical schemes that preserve the permutation identity and hence the energy and helicity numerically. By construction, EHPS is nonlinearly stable and free from excess numerical viscosity, and suitable for long time integration. We also give a clean way of handling geometric singularities on the axis of rotation for axisymmetric flows.

The procedure is quite general. Any type of spatial discretization such as finite difference, finite element, and spectral methods can be treated similarly by numerically realizing the permutation identity (4.5). Local mesh refinement near the physical boundary can also be incorporated into the scheme by stretching the coordinate accordingly at no extra cost. Numerical evidence has demonstrated both accuracy and efficiency of the scheme.

Acknowledgements

This work was initialized when both authors were visiting the National Center for Theoretical Sciences in Taiwan. We thank the faculty and staff there for their warm hospitality. J.G. Liu is also sponsored in part by NSF grant DMS-0107218. W.C. Wang is sponsored in part by NSC of Taiwan under grant number 90-2115-M-007-024.

Appendix A

A.1. Energy and helicity identities for MHD flows with symmetry

We have derived the two conservation laws (2.10) and (2.11) in Section 2 using the fact that the nonlinear term $\boldsymbol{\omega} \times \boldsymbol{u}$ is perpendicular to both $\boldsymbol{\omega}$ and $\boldsymbol{u}$. This is a special case of the following vector identity:

$$\boldsymbol{f} \times \boldsymbol{g} \cdot \boldsymbol{h} = \boldsymbol{g} \times \boldsymbol{h} \cdot \boldsymbol{f} = \boldsymbol{h} \times \boldsymbol{f} \cdot \boldsymbol{g}, \qquad \boldsymbol{f} \times \boldsymbol{g} \cdot \boldsymbol{h} = -\boldsymbol{g} \times \boldsymbol{f} \cdot \boldsymbol{h}. \tag{A.1}$$

In view of the nonlinear terms in the MHD equation (2.3), it is convenient to introduce the vector potential formulation for the Faraday equation first:

$$\partial_t \boldsymbol{b} = -\eta \nabla \times \boldsymbol{j} + \nabla \times (\boldsymbol{u} \times \boldsymbol{b}). \tag{A.2}$$

Since the right hand side of (A.2) is divergence free, it is clear that $\nabla \cdot \boldsymbol{b} = 0$ as long as $\nabla \cdot \boldsymbol{b}|_{t=0} = 0$. We can therefore find a vector potential $\boldsymbol{a}$ such that $\nabla \times \boldsymbol{a} = \boldsymbol{b}$. Moreover,

$$\nabla \times (\partial_t \boldsymbol{a} + \eta \boldsymbol{j} - \boldsymbol{u} \times \boldsymbol{b}) = \boldsymbol{0} \tag{A.3}$$

and

$$\partial_t \boldsymbol{a} = -\eta \boldsymbol{j} + \boldsymbol{u} \times \boldsymbol{b} - \nabla \chi, \tag{A.4}$$

with a gauge function χ.

Therefore the MHD equation can be written as

$$\partial_t \boldsymbol{u} + \boldsymbol{\omega} \times \boldsymbol{u} + \nabla \tilde{p} = -\nu \nabla \times \boldsymbol{\omega} + \alpha \boldsymbol{j} \times \boldsymbol{b}, \tag{A.5}$$

$$\partial_t \boldsymbol{a} + \boldsymbol{b} \times \boldsymbol{u} + \nabla \chi = -\eta \nabla \times \boldsymbol{b}, \tag{A.6}$$

where $\boldsymbol{\omega} = \nabla \times \boldsymbol{u}$, $\boldsymbol{b} = \nabla \times \boldsymbol{a}$, $\boldsymbol{j} = \nabla \times \boldsymbol{b}$ and $\nabla \cdot \boldsymbol{u} = 0$.

At this point, it is quite straight forward to derive all the conserved quantities by managing to cancel the nonlinear terms in (A.5) and (A.6) using (A.1).

The conservation of energy is given by taking the inner product of (A.5) with $\boldsymbol{u}$ and the inner product of (A.6) with $\alpha \boldsymbol{j}$:

$$\frac{\mathrm{d}}{\mathrm{d}t} \frac{1}{2} \int_D (|\boldsymbol{u}|^2 + \alpha |\boldsymbol{b}|^2) = -\nu \int_D |\boldsymbol{\omega}|^2 - \alpha \eta \int_D |\boldsymbol{j}|^2. \tag{A.7}$$

The conservation of the cross helicity is given by taking the inner product of (A.5) with $\boldsymbol{b}$ and the inner product of (A.6) with $\boldsymbol{\omega}$:

$$\frac{\mathrm{d}}{\mathrm{d}t} \int_D \boldsymbol{u} \cdot \boldsymbol{b} + \int_{\partial D} \tilde{p} \boldsymbol{b} \cdot \boldsymbol{n} = -\nu \int_D \boldsymbol{b} \cdot (\nabla \times \boldsymbol{\omega}) - \eta \int_D \boldsymbol{\omega} \cdot \boldsymbol{j}, \tag{A.8}$$

where in both (A.7) and (A.8), we have used the boundary conditions (2.4) and the identity (2.7).

An alternative expression to (A.8) can be derived by taking the inner product of $\boldsymbol{a}$ with the curl of (A.5) and the inner product of $\boldsymbol{u}$ with the curl of (A.6) and proceed as before. The result is given by

$$\frac{\mathrm{d}}{\mathrm{d}t} \int_D \boldsymbol{u} \cdot \boldsymbol{b} = -\nu \int_D \boldsymbol{a} \cdot (\nabla \times \nabla \times \boldsymbol{\omega}) - \eta \int_D \boldsymbol{\omega} \cdot \boldsymbol{j}. \tag{A.9}$$

The magnetic helicity $\frac{1}{2}\int_D \boldsymbol{a}\cdot\boldsymbol{b}$ in general depends on the choice of the gauge χ. If we restrict ourselves to the subclass $\chi|_{\partial D}=0$, then the magnetic helicity is gauge invariant. The conservation of magnetic helicity can be derived by taking the inner product of (A.6) with $\boldsymbol{b}$:

$$\frac{1}{2}\frac{\mathrm{d}}{\mathrm{d}t}\int_D \boldsymbol{a}\cdot\boldsymbol{b} = -\eta\int_D \boldsymbol{b}\cdot\boldsymbol{j}. \tag{A.10}$$

Following the procedure outlined in (3.23)–(3.30), we can similarly express (A.7), (A.9) and (A.10) in terms of the computational variables as

$$\frac{\mathrm{d}}{\mathrm{d}t}\frac{1}{2}(\langle u,u\rangle + [\psi,\psi] + \alpha\langle b,b\rangle + \alpha[a,a]) + \nu([u,u] + \langle\omega,\omega\rangle) + \eta\alpha([j,j] + \langle b,b\rangle) = 0, \tag{A.11}$$

$$\frac{\mathrm{d}}{\mathrm{d}t}(\langle u,b\rangle + \langle\omega,a\rangle) = \nu(\langle b,(\nabla^2 - V)u\rangle + \langle a,(\nabla^2 - V)\omega\rangle) + \alpha\eta\big([u,b] + \langle\omega,(\nabla^2 - V)a\rangle\big) \tag{A.12}$$

and

$$\frac{\mathrm{d}}{\mathrm{d}t}\langle a,b\rangle + \eta[a,b] = 0. \tag{A.13}$$

A.2. Discrete energy and helicity identities for Navier–Stokes equation with physical boundaries

Here we show that the discrete permutation identity (4.14) remains valid in the presence of physical boundary for axisymmetric flows. We first introduce the convolution operator

$$(f*g)_{i-\frac{1}{2}} = \tfrac{1}{2}(f_{i-1}g_i + f_i g_{i-1}),$$

we can write (5.9) as

$$\sum_{i=1}^{M-1} f_i(g_{i+1} - g_{i-1}) = -\sum_{i=1}^{M-1}(f_{i+1} - f_{i-1})g_i + 2(f*g)_{M-\frac{1}{2}} - 2(f*g)_{\frac{1}{2}}, \tag{A.14}$$

therefore

$$\begin{aligned}\Delta x\Delta r\sum_j\sum_{i=1}^{M-1}\Big(c\tilde{D}_x(a\tilde{D}_r b)\Big)_{i,j} = &-\Delta x\Delta r\sum_j\sum_{i=1}^{M-1}\Big(a(\tilde{D}_x c)(\tilde{D}_r b)\Big)_{i,j}\\ &+\Delta r\left(\sum_j (c *_x a\tilde{D}_r b)_{M-\frac{1}{2},j} - (c *_x a\tilde{D}_r b)_{\frac{1}{2},j}\right),\end{aligned} \tag{A.15}$$

where $*_x$ denotes convolution in x direction. Similarly,

$$\begin{aligned}\Delta x\Delta r\sum_i\sum_{j=1}^{N-1}\Big(c\tilde{D}_r(a\tilde{D}_x b)\Big)_{i,j} = &-\Delta x\Delta r\sum_i\sum_{j=1}^{N-1}\Big(a(\tilde{D}_r c)(\tilde{D}_x b)\Big)_{i,j}\\ &+\Delta x\left(\sum_i (c *_r a\tilde{D}_x b)_{i,N-\frac{1}{2}} - (c *_r a\tilde{D}_x b)_{i,\frac{1}{2}}\right).\end{aligned} \tag{A.16}$$

From (A.15) and (A.16) it follows that

$$\Delta x\Delta r\sum_{i,j} c\tilde{\nabla}_h\cdot(a\tilde{\nabla}_h^{\perp}b) = -\Delta x\Delta r\sum_{i,j} a\tilde{\nabla}_h c\cdot\tilde{\nabla}_h^{\perp}b - \Delta y_\tau\sum_{\Gamma_h}\Big(c *_n (a\tilde{D}_\tau b)\Big), \tag{A.17}$$

$$\Delta x\Delta r\sum_{i,j} c\tilde{\nabla}_h^{\perp}\cdot(b\tilde{\nabla}_h a) = -\Delta x\Delta r\sum_{i,j} b\tilde{\nabla}_h^{\perp}c\cdot\tilde{\nabla}_h a + \Delta y_\tau\sum_{\Gamma_h}\Big(c *_n (b\tilde{D}_\tau a)\Big), \tag{A.18}$$

where for brevity, we have used $*_n$ to denote the convolution in the normal direction and y_τ the variable in the tangential direction.

We have the discrete analogue of (4.3):

$$\begin{aligned}\sum_{i,j} cJ_h(a,b)\Delta x\Delta r = {} & \sum_{i,j}(c\tilde{\nabla}_h a\cdot\tilde{\nabla}_h^{\perp}b + a\tilde{\nabla}_h b\cdot\tilde{\nabla}_h^{\perp}c + b\tilde{\nabla}_h c\cdot\tilde{\nabla}_h^{\perp}a)\Delta x\Delta r\\ & + \frac{1}{3}\sum_{\Gamma_h}\Big(c *_n (a\tilde{D}_\tau b - b\tilde{D}_\tau a)\Big)\Delta y_\tau.\end{aligned} \tag{A.19}$$

For the discrete energy identity (4.23), the boundary contribution from the 3 nonlinear terms

$$\frac{1}{3}\sum_{\Gamma_h}\Big(c *_n (a\tilde{D}_\tau b - b\tilde{D}_\tau a)\Big) \tag{A.20}$$

corresponds to $(a,b,c) = (h_3u, h_3\psi, u/h_3)$, $(\omega/h_3, h_3\psi, h_3\psi)$ and $(u/h_3, h_3u, h_3\psi)$, respectively. From (5.11), the convolutions involving ψ drop out automatically. For the same reason, the only boundary contribution from the nonlinear terms in the derivation of the discrete helicity identity corresponds to $(a,b,c) = (u/h_3, h_3u, h_3u)$. This term is also identically zero since on $r = r_{\max}$, we have

$$(a\tilde{D}_\tau b - b\tilde{D}_\tau a) = (u\tilde{D}_x u - u\tilde{D}_x u) = 0 \quad \text{on } j = N-1, N,$$

while on $x = x_{\min}$ and $x = x_{\max}$,

$$\Big(c *_n (a\tilde{D}_\tau b\Big) = r\Big(u *_x (u/r\tilde{D}_r(ru)\Big) = 0$$

and

$$\Big(c *_n (b\tilde{D}_\tau a)\Big) = r\Big(u *_x ru\tilde{D}_r(u/r))\Big) = 0$$

from (5.12).

In the mean time, we have the following Lemma 1 concerning the boundary contributions for the viscous term.

Lemma 1. *If either a satisfies the homogeneous Dirichlet boundary condition*

$$a_{0,j} + a_{1,j} = 0, \quad a_{M-1,j} + a_{M,j} = 0, \quad a_{i,N-1} + a_{i,N} = 0$$

or b satisfies the homogeneous Neumann boundary condition

$$b_{0,j} = b_{1,j}, \quad b_{M-1,j} = b_{M,j}, \quad b_{i,N-1} = b_{i,N}$$

at the physical boundary, then

$$\langle a, (\nabla_h^2 - V)b\rangle_h = -[a,b]_h. \tag{A.21}$$

The proof follows straight forward from the following identity

$$\sum_{i=1}^{M-1} f_i(g_{i+1/2} - g_{i-1/2}) = -\sum_{i=1}^{M}{}' (f_i - f_{i-1})g_{i-1/2} + \frac{1}{2}(f_{M-1} + f_M)g_{M-1/2} - \frac{1}{2}(f_1 + f_0)g_{1/2}, \tag{A.22}$$

where

$$\sum_{i=1}^{M}{}' = \frac{1}{2}\sum_{i=1} + \sum_{i=2}^{M-1} + \frac{1}{2}\sum_{i=M}.$$

From the analysis above, we see that the energy and helicity identities (4.23) and (4.24) remains valid with the physical boundary condition (5.11) and (5.12).

References

[1] A. Arakawa, Computational design for long-term numerical integration of the equations of fluid motion: two dimensional incompressible flow. Part I, J. Comput. Phys. 1 (1966) 119–143.
[2] L. Caffarelli, R. Kohn, L. Nirenberg, Partial regularity of suitable weak solutions of the Navier–Stokes equations, Commun. Pure Appl. Math. 35 (1982) 771–831.
[3] W. E, J.-G. Liu, Vorticity boundary condition and related issues for finite difference schemes, J. Comput. Phys. 124 (1996) 368–382.
[4] H. Friedel, R. Grauer, C. Marliani, Adaptive mesh refinement for singular current sheets in incompressible magnetohydrodybnamic flows, J. Comput. Phys. 134 (1997) 190–198.
[5] R. Grauer, T.C. Sideris, Numerical computation of 3D incompressible ideal fluids with Swirl, Phys. Rev. Lett. 67 (1991) 3511–3514.
[6] F.H. Harlow, J.E. Welch, Numerical calculation of time-dependent viscous incompressible flow of fluid with free surface, Phys. Fluids 8 (1965) 2182–2189.
[7] C.D. Levermore, J.-G. Liu, Large oscillations arising from a dispersive numerical scheme, Physica D 99 (1996) 191–216.
[8] J.-G. Liu, C.-W. Shu, A high order discontinuous Galerkin method for incompressible flows, J. Comput. Phys. 160 (2000) 577–596.
[9] J.-G. Liu, W.C. Wang, An energy preserving MAC–Yee scheme for the incompressible MHD equation, J. Comput. Phys. 174 (2001) 12–37.
[10] J.-G. Liu, W.C. Wang, Convergence analysis of energy and helicity preserving schemes for axisymmetric flows, preprint.
[11] J.-G. Liu, Z. Xin, Convergence of a Galerkin method for 2-D discontinuous Euler flows, Commun. Pure Appl. Math. 53 (2000) 786–798.
[12] P.E. Merilees, The pseudospectral approximation applied to the shallow water equations on a sphere, Atmosphere 11 (1973) 13–20.
[13] H.K. Moffatt, A. Tsinober, Helicity in laminar and turbulent flow, Ann. Rev. Fluid Mech. 24 (1992) 281–312.
[14] J.J. Moreau, Constantes d'unîlot tourbillionnaire en fluide parfait barotrope, C.R. Acad. Sci. Paris 252 (1961) 2810–2812.
[15] S.A. Orszag, M. Israeli, Numerical simulation of viscous incompressible flows, Ann. Rev. Fluid Mech. 6 (1974) 281–318.
[16] A. Thom, The flow past circular cylinders at low speeds, Proc. R. Soc. London A 141 (1933) 651–669.
[17] K. Yee, Numerical solution of initial boundary value problems involving Maxwell's equations in isotropic media, IEEE Trans. Antennas Propagation AP-16 (1966) 302–307.